

Dynamic behavior of suspended sediment concentrations in a shallow lake perturbed by episodic wind events

Richard A. Luettich, Jr.

University of North Carolina Institute of Marine Sciences, 3407 Arendell St., Morehead City 28557

Donald R. F. Harleman

R. M. Parsons Laboratory, Massachusetts Institute of Technology, Cambridge 02139

László Somlyódy

Research Centre for Water Resources Development, Budapest, Hungary

Abstract

Field experiments were conducted in Lake Balaton, a large (surface area, 600 km²) but shallow (mean depth, 3.2 m) lake in Hungary, to quantify the resuspension and deposition of bottom sediment due to episodic storm events. Measurements were made of windspeed and direction, surface waves, mean water velocity, and suspended sediment concentration. During significant wind events, the computed bottom stress due to surface waves dominated that due to the mean current, and therefore surface waves were assumed to be the major cause of sediment resuspension. A simple model for the depth-averaged suspended sediment concentration based on surface wave height was calibrated with about 10 h of data collected during one storm event and verified against 15 d of data collected at the same site. The success of the suspended sediment model, which assumes that the bottom sediment was noncohesive, is surprising since the bottom material was composed predominantly of sediment in the clay and fine-silt size ranges. This fit may indicate the presence of a thin surface layer of loosely bound sediment that is continuously involved in resuspension. The suspended sediment model could easily be integrated into a water quality model (e.g. to predict light attenuation), provided that lateral transport is negligible, or it could be used to provide the bottom boundary condition for a more general suspended sediment transport model in which advective transport is included.

Due to their small fall velocities, fine-grained particles (i.e. those in the silt and clay size ranges) are transported easily by flows. An understanding of the dynamic behavior of these particles is particularly important in shallow lakes and estuaries since there they may repeatedly settle to the bot-

tom and be resuspended throughout the water column.

Lake Balaton, Hungary, is an example of a shallow body of water that is significantly affected by fine-grained suspended sediment. This lake has the largest surface area of any lake in central Europe (about 600 km²) but has a mean depth of only 3.2 m (Fig. 1). A recent survey of the bottom sediment by Máté (unpubl.) has shown that it consists primarily of fine silt and clay except near the southern shore and in the Tihany Straits where coarser fractions prevail. The water quality in the lake is affected by resuspension and settling of these sediments in at least two ways. First, sediments suspended in the water column decrease light penetration, yielding Secchi disk depths that can be 20 cm or less and rarely are as much as 1 m. In the hypertrophic western end of the lake there is evidence that in summer light limits phytoplankton growth (Luettich and Harleman 1986). Second, the sediments are capable of acting as an internal

Acknowledgments

This work was supported jointly by the National Science Foundation and the Hungarian Academy of Science under the U.S.-Hungary Cooperative Science Program (grants INT 81-12454 and INT 84-11545) and by the National Science Foundation Environmental Engineering Program (grant ECE 82-11525).

Sandy Williams and Dick Koehler spent many hours making BASS work with the instrumentation system. The fieldwork at Lake Balaton would have been impossible without the help of many of the staff members at the Limnological Research Institute of the Hungarian Academy of Sciences and at the Hungarian Research Centre for Water Resources Development. Suggestions made by W. B. Dade, J. W. Lavelle, and an anonymous reviewer improved this paper and are acknowledged.

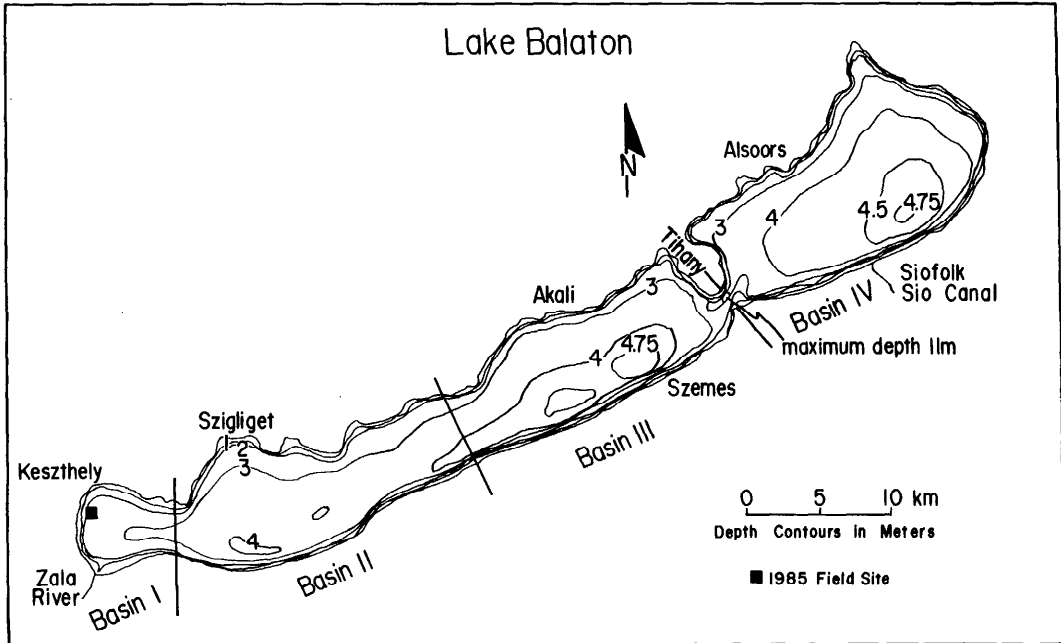


Fig. 1. Lake Balaton, Hungary.

source of nutrients because as much as 95% of the external supply of P to the lake is retained in the bottom sediments. Lijklema et al. (1986) found orthophosphorus concentrations in Lake Balaton sediments that were two orders of magnitude greater than in the overlying lake water. Experimental work by Gelencsér et al. (1982) showed that the desorption of P from bottom sediments resuspended by even a moderate storm could be comparable in magnitude to the daily average external supply. This internal source of nutrients may be particularly important to Lake Balaton, since in 1983 a comprehensive P reduction program was launched covering the entire watershed of the lake (Láng 1986).

As a component of a larger effort to address the effects of sediment on water quality in the lake (Somlyódy and van Straten 1986), the objective of the present study was to develop a model to predict storm-induced changes in the suspended sediment concentration of the lake. This paper presents the results of a field program to measure the hydrodynamic and sediment response of the lake to storm events and the

development and application of a model for the suspended sediment concentration.

Field study

Instrumentation—A field study was conducted in water 2 m deep about 300 m from the western end of the lake (Fig. 1) from 6–21 August 1985. Suspended sediment concentrations were determined gravimetrically with middepth water samples collected from a boat anchored at the field site. Sampling was accomplished by lowering an empty 1-liter bottle to the desired depth and subsequently opening a vent tube that ran to the surface. This permitted water to enter the bottle through a sampling port as the air escaped through the vent tube. Samples were taken every 2–3 h during an initial storm and subsequent calm periods and as often as every 10 min during a second storm. Windspeed and direction were recorded continuously at a land-based meteorological station about 500 m from the site.

Additional data were collected from a tripod-based system of instruments that included windspeed and direction sensors mounted 2 m above the mean water level

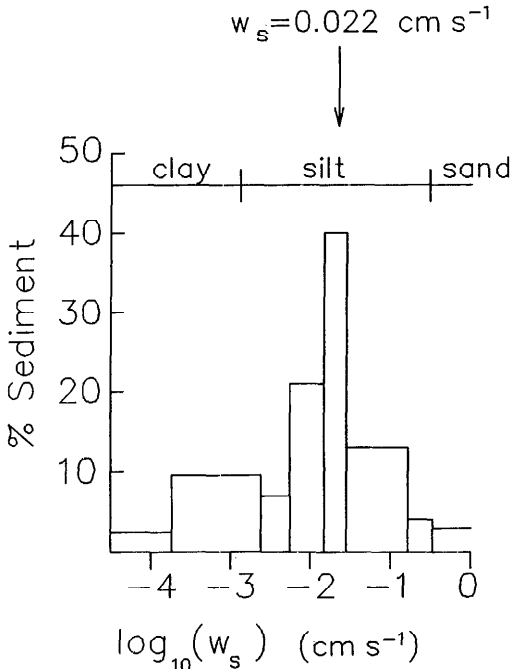


Fig. 2. Settling velocities of surface sediment collected at the field site.

and two BASS velocity meters located 24 and 85 cm above the bottom. BASS is an acoustic time-of-travel sensor that is capable of resolving water velocity in three dimensions to 0.03 cm s^{-1} (based on a 12-bit analog to digital conversion) and has an accuracy of 0.3 cm s^{-1} (limited by the repeatability of velocity measurements in still water) (Williams 1985). The distance from each BASS sensor to the bottom was measured in situ 5 d after the tripod was deployed and therefore accounts for initial tripod settling into the sediments. Subsequent measurements indicated that further settling was negligible.

A remote-control assembly that consisted of a C.B. radio and a tone-decoding circuit was mounted on the wind sensor mast. It allowed the instruments to be turned on and off and the sampling rate to be varied by sending different tone sequences over the radio.

Results—Settling-column analyses of bottom material collected by a diver indicated that the surface sediment consisted principally of clay and fine silt (Fig. 2). Plots

of windspeed and direction from the meteorological station show that two major storms (beginning at about 0000 hours on 7 August and 2200 hours on 17 August) occurred during the study period. Each storm had northerly winds with hourly averaged speeds of $7\text{--}9 \text{ m s}^{-1}$ (Fig. 3a). These events were responsible for increasing the middepth suspended sediment concentration from a background level of about 15 mg liter^{-1} to maximum concentrations $>150 \text{ mg liter}^{-1}$ (Fig. 3b).

Unfortunately, the tripod-based instruments could not be deployed until after the first storm. Also, many of the data collected while the instruments were deployed were lost due to a corroded connector between the data-logger housing and the housing containing the cassette tape used for data storage. Data were recorded successfully, however, for about 61 h from 2000 hours on 15 August to 0800 hours on 18 August, the final 10 h corresponding to the second storm. Data were collected at 2 Hz, although to conserve cassette tape they were taken in 6-min bursts once every hour, 30 min, or 15 min, depending on prevailing conditions.

Two small wind events during which the wind blew from east to west along the long axis of the lake were followed by the second major storm (Fig. 4a). Winds during the storm were oriented from north to south across the lake and were almost twice as strong as during the smaller events.

The vertical component of the velocity measured by the upper BASS was used to compute statistical wave properties. Extensive comparisons between the one-dimensional velocity spectra measured by the upper and lower BASS showed that linear wave theory accurately described velocities in the surface-wave band of the spectra for significant wave heights $\geq 4 \text{ cm}$. Therefore linear theory was used to extrapolate vertical velocity spectra from the upper BASS into wave-height spectra at the surface. The wave-height spectra were then used to determine significant wave heights with assumptions for narrow-banded wave spectra (Ochi 1982). Reliable separation between wave velocities and turbulent velocities could not be obtained at significant wave

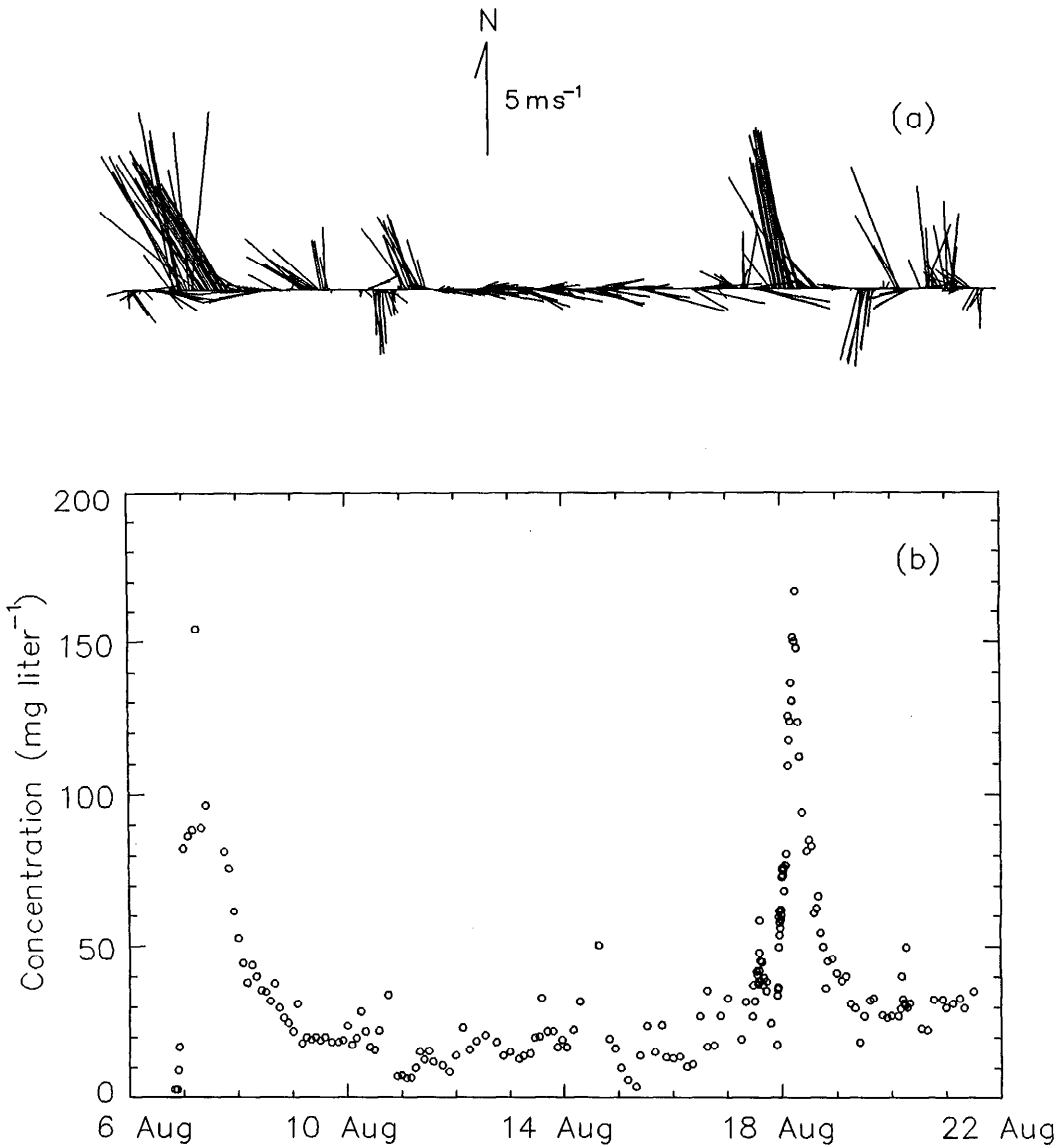


Fig. 3. a. The 30-min-averaged wind velocity measured at the Keszthely meteorological station during the 15-d field study. (Vectors point in the direction the wind is blowing from.) b. Observed middepth suspended sediment concentrations during the 15-d field study.

heights ≤ 4 cm—therefore taken as a lower cutoff. During the two small events, significant wave heights reached ~ 17 cm, during the major storm they reached 25 cm (Fig. 4b). The mean period was relatively constant during each wind event at a value of ~ 2 s (Fig. 4c).

The current in the lower 85 cm of the

water column was typically parallel to shore with maximal speeds of $10\text{--}12 \text{ cm s}^{-1}$ (Fig. 5a,b). Although the two small wind events were similar in strength and direction, the corresponding horizontal water velocities were in opposite directions. It appears that in each case winds blowing along the lake enhanced the existing mean current at the

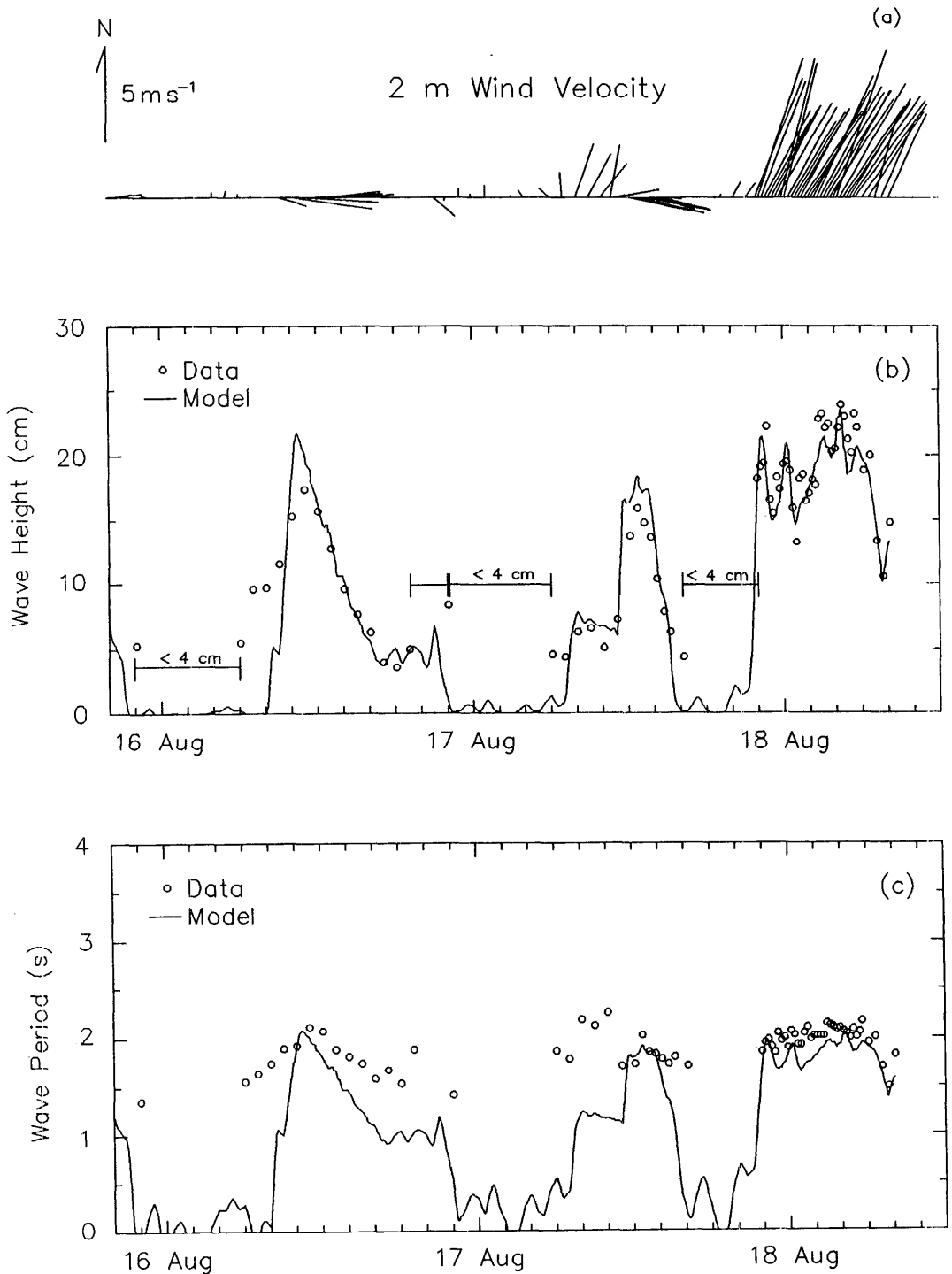


Fig. 4. a. Wind velocity measured by the tripod-based instruments computed by averaging during each 6-min sampling burst. (Vectors point in the direction the wind is blowing from.) b. Observed and modeled significant wave heights. c. Observed mean wave period (defined as the ratio of the zeroth to the first-order moment of the wave-height spectrum) and modeled significant wave period.

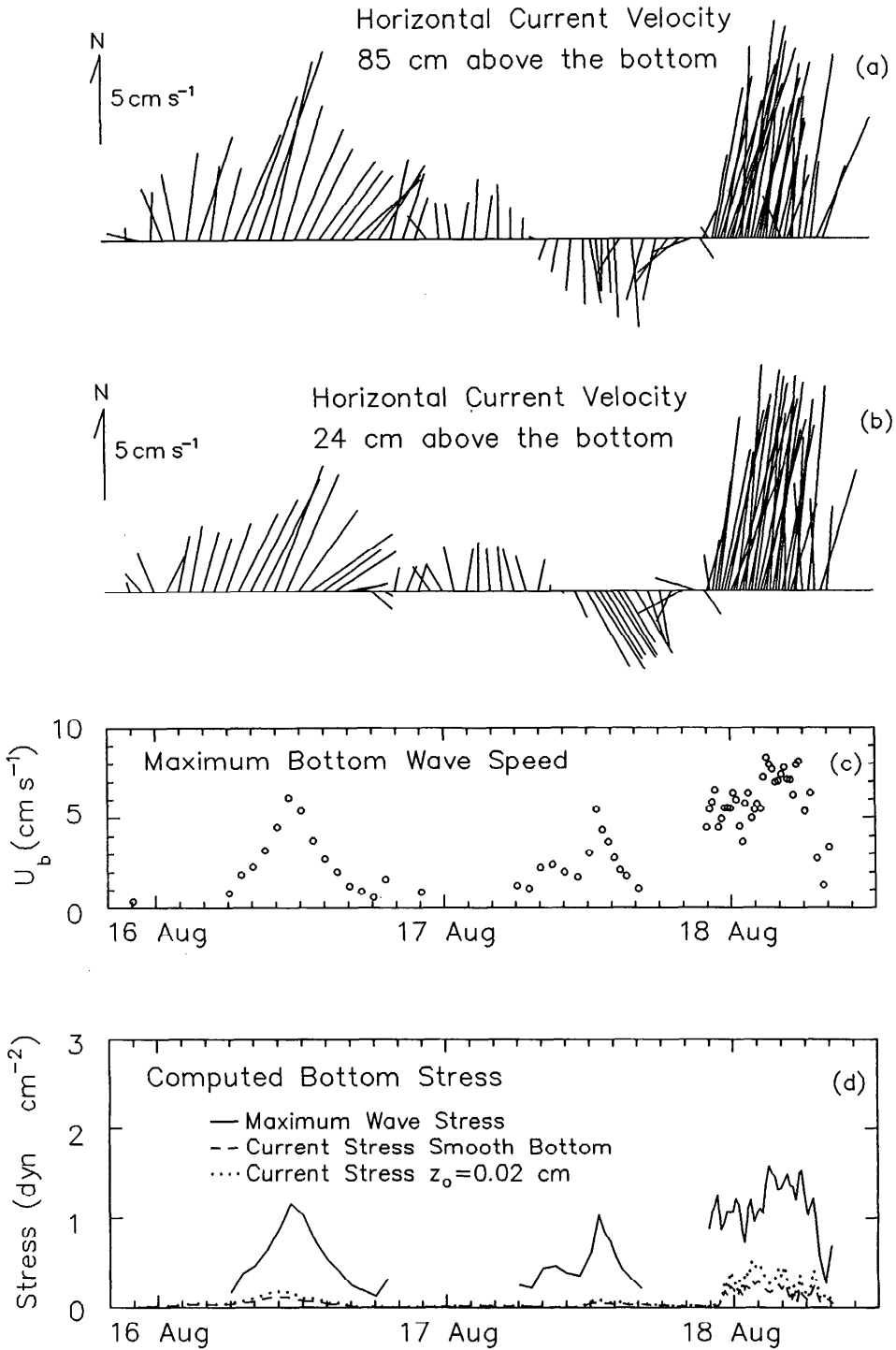


Fig. 5. a, b. Horizontal current velocity measured 85 and 24 cm above the bottom. (Vectors point in the direction the current is flowing toward.) c. Computed maximal, wave-induced orbital velocity at the bottom. d. Computed bottom stress due to the waves and current.

Significant symbols

A_b	Maximum bottom wave excursion amplitude (cm)
c	Suspended sediment concentration (mg liter ⁻¹)
\bar{c} , c_{bak} , c_c	Depth-averaged, nonsettling background, and equilibrium suspended sediment concentrations (mg liter ⁻¹)
E	Sediment pickup rate (g cm ⁻² s ⁻¹)
f_w	Wave friction factor
F	Effective fetch (m)
g	Acceleration of gravity (=9.81 m s ⁻²)
h	Water depth (m)
H	Wave height (cm)
H_c , H_{ref} , H_s	Critical, reference, and significant wave heights (cm)
k	Wave number (m ⁻¹)
K	Model parameter (mg liter ⁻¹)
L	Length scale over which there is significant variation in c (km)
n	Model parameter
t	Time (s)
Re_w	Wave Reynolds number
T	Wave period (s)
T_c	Time scale for a significant change in c (min)
T_h	Horizontal transport time scale (h)
u , v , w	Water velocity components in the x , y , z directions
U	Mean advective velocity scale (cm s ⁻¹)
U_b	Maximum bottom wave orbital velocity (cm s ⁻¹)
$U_{\text{curr}}(z)$	Mean current velocity (cm s ⁻¹)
U_{curr}	Mean current friction velocity (cm s ⁻¹)
w_s	Particle settling velocity (cm s ⁻¹)
W_{10}	Windspeed measured 10 m above the water surface (m s ⁻¹)
x , y	Horizontal coordinate directions
z	Vertical coordinate direction, positive upward, $z = 0$ at still water
z_0	Bottom roughness (cm)
α , ζ , γ , δ	Wave model constants
β	Model settling parameter (cm s ⁻¹)
Δt	Model time step (s)
κ	Von Kármán constant (=0.4)
λ	Wavelength (m)
ν	Kinematic viscosity of water (=0.01 cm ² s ⁻¹)
ω	Wave frequency (s ⁻¹)
ρ	Density of water (=1 g cm ⁻³)
τ	Bottom stress (dyn cm ⁻²)
τ_c	Critical bottom stress (dyn cm ⁻²)
τ_{curr}	Bottom stress due to mean current (dyn cm ⁻²)
τ_{ref}	Reference bottom stress (dyn cm ⁻²)
τ_{wave}	Maximum bottom stress during a wave cycle (dyn cm ⁻²)
ϕ	Vertical sediment flux at the bottom (g cm ⁻² s ⁻¹)

measurement site. The direction of this current was probably determined by the seiching motion of the lake and by the previous wind history. During the major storm, the near-bottom current was directed toward the north, indicating a transverse setup in the lake, with a bottom return current against the wind.

Estimates of bottom stress due to the mean current and due to the surface waves were made to guide development of the sediment resuspension model. If the wave and current boundary layers are turbulent, the bottom stress is a highly nonlinear function of the near-bottom current velocity and the bottom wave orbital velocity (Smith 1977; Grant and Madsen 1979). Calculations for the 61 h of wave data indicate, however, that the wave boundary layer was probably viscous dominated (i.e. in the laminar regime as shown in Kamphius 1975, figure 9). In this case the wave and bottom stress can be treated separately.

The bottom stress associated with the mean current is

$$\tau_{\text{curr}} \equiv \rho U_{* \text{curr}}^2 \quad (1)$$

(Units given in list of symbols.) If the mean velocity profile is logarithmic near the bottom, $U_{* \text{curr}}$ can be calculated from measurements of mean current velocity with

$$U_{* \text{curr}} = \frac{\kappa U_{\text{curr}}(z)}{\ln(z/z_0)} \quad (2)$$

It was not possible to determine the hydraulic bottom roughness from the field measurements with adequate precision and therefore two estimates were used in Eq. 2, $z_0 = 0.02$ cm and $z_0 = \nu/9U_{* \text{curr}}$. The former value for z_0 is recommended over a mud bottom by Soulsby (1983) and is consistent with the value of $z_0 = 0.016$ cm obtained over a bottom of fine-grained sediment at the HEBBLE site during and after a storm (Gross et al. 1986). The latter value of z_0 comes from laboratory experiments over a smooth boundary (Monin and Yaglom 1971). Its use may be appropriate for our data because of the fine-grained bottom sediment and because daily dives at the field site revealed no discernible physically or bi-

ologically induced bedforms. τ_{curr} was calculated with the 6-min-averaged velocity measured by the lower BASS and therefore assumes that a logarithmic layer extended 24 cm above the bed.

Maximal bottom stress during a wave cycle can be computed as

$$\tau_{\text{wave}} = \frac{f_w}{2} \rho U_b^2. \quad (3)$$

(Summaries of Eq. 3–5 are found elsewhere: Sleath 1984; Dyer 1986.) In a viscous-dominated, wave boundary layer

$$f_w = 2(\text{Re}_w)^{-1/2} \quad (4)$$

where Re_w is defined as

$$\text{Re}_w \equiv \frac{U_b A_b}{\nu}. \quad (5)$$

It appears (Fig. 5d) that τ_{wave} dominates τ_{curr} by a factor ranging from 4 to 10, depending on which value of bottom roughness is used. The dominance of τ_{wave} over τ_{curr} occurs because bottom shear is proportional to the velocity gradient in the boundary layer. The current boundary layer has a characteristic period on the order of hours and therefore it can grow to a thickness comparable to the depth of the water column. Because surface waves have periods of only a few seconds, however, the wave boundary layer does not have a chance to grow to a thickness of more than a few millimeters. As a result the same bottom stress can be generated by wave-induced bottom orbital velocities that are much smaller than the mean current velocity. Since the bottom orbital velocity and the mean current velocity are typically of the same order of magnitude in Lake Balaton (e.g. Fig. 5a–c), it may be reasonable to neglect the stress due to the mean current in comparison with that due to the waves when specifying the forcing responsible for eroding bottom sediments. This conclusion is consistent with field data reported by Anderson (1972) for floodtides over a tidal flat, by Lesht et al. (1980) on the Long Island inner continental shelf, and by Carper and Bachmann (1984) in a small prairie lake—each of whom found that concentrations of

fine particles in suspension were correlated with the presence of surface waves.

Suspended sediment model development

For conditions typically encountered in nature, the suspended sediment concentration can be modeled with a three-dimensional mass transport balance:

$$\begin{aligned} \frac{\partial \bar{c}}{\partial t} + \frac{\partial}{\partial x} [\overline{uc}] + \frac{\partial}{\partial y} [\overline{vc}] + \frac{\partial}{\partial z} [(\bar{w} - w_s)\bar{c}] \\ = -\frac{\partial}{\partial x} [\overline{u'c'}] - \frac{\partial}{\partial y} [\overline{v'c'}] - \frac{\partial}{\partial z} [\overline{w'c'}]. \end{aligned} \quad (6)$$

Molecular diffusion terms in Eq. 6 have been dropped in comparison with their turbulent counterparts.

If the total suspended sediment concentration is modeled with a single mass transfer equation, w_s can be expected to vary as a function of time due to changes in the particle size distribution. Such changes may occur because of differential settling and flocculation/deflocculation in the water column. Alternatively, the total suspended sediment concentration can be broken up into different size classes, each of which has its own transport equation and w_s (e.g. see Hawley 1983; McLean 1985; Lick 1986). With this approach, differential settling is modeled explicitly while flocculation and deflocculation are treated by including source-sink terms in the transport equation for each size class.

In laboratory experiments Krone (unpubl. rep.) found that discrete particle settling occurred for mud taken from San Francisco Bay at suspended sediment concentrations $< 300 \text{ mg liter}^{-1}$. Similarly Lee et al. (1981) found that the effects of flocculation were small for suspensions of Lake Erie sediments in freshwater at concentrations $< 500 \text{ mg liter}^{-1}$, while van Leussen (1986) found no effect of flocculation for suspensions of kaolinite in freshwater at concentrations of 50 mg liter^{-1} . On the basis of these results, the effects of flocculation and deflocculation in the water column are expected to have a negligible effect on the size distribution of suspended particles in Lake Balaton. Due to a lack of data on temporal variations in the particle size distri-

bution in the lake, the total suspended sediment concentration was modeled by a single equation with constant w_s .

Equation 6 can be simplified for use in the present study by considering time scales that pertain to the Keszthely field site. If we assume that horizontal advection dominates horizontal turbulent diffusion, a time scale for the horizontal transport of suspended sediment can be expressed as $T_h \sim L/U$. Based on the velocities presented in Fig. 5a,b and a circulation study done by Shanahan and Harleman (1982), it is assumed that away from Tihany Straits, $U \sim 5 \text{ cm s}^{-1}$. L depends on spatial variability in the bottom sediment properties and the applied forcing. Bottom sediment properties typically vary on scales of 1–5 km and larger (Máté unpubl.). Principal forcing appears due to surface waves (Fig. 5d). Winds blowing from the north across the lake have fetches at the field site of about 2.5 km and therefore a value of $L \sim 1 \text{ km}$ might be appropriate. Due to the long fetch, waves generated by winds blowing along the long axis of the lake have $L \gg 1 \text{ km}$. Györke (unpubl. rep.) made transects across Keszthely Bay during a storm and found less than a factor of two difference in suspended sediment concentration, suggesting that $L \gg 1 \text{ km}$. Even with the most conservative value of L , we estimate that $T_h \sim 6 \text{ h}$ or more.

Most of the time-significant variations in the middepth suspended sediment concentration occur on time scales of $T_c \sim 30 \text{ min}$ (Fig. 3). Since $T_c \ll T_h$, these concentration changes must be due to vertical fluxes rather than horizontal advection. The only exceptions occur near the end of prolonged periods of settling which follow major re-suspension events. With this possible limitation, the horizontal advective and diffusive transport terms are dropped from Eq. 6, leaving

$$\frac{\partial \bar{c}}{\partial t} + \frac{\partial}{\partial z} [(\bar{w} - w_s)\bar{c}] = -\frac{\partial}{\partial z} [\overline{w'c'}]. \quad (7)$$

Vertical profiles collected in Keszthely Bay by Györke (unpubl. rep.), near Szemes by Somlyódy (1982), and near Tihany by Luet-

tich (1987) all indicate that suspended sediment concentrations are nearly uniform in the vertical. Physically, this pattern is due to the small particle sizes in suspension and the shallowness of the lake, which allows turbulence to penetrate easily throughout the depth. The lack of a significant vertical concentration gradient makes it convenient to model the depth-averaged suspended sediment concentration. Integrating Eq. 7 over the water column with the assumptions of a constant depth and no sediment flux at the free surface yields

$$h \frac{d\tilde{c}}{dt} = \phi \quad (8)$$

where \tilde{c} and ϕ are defined as

$$\tilde{c} \equiv \frac{1}{h} \int_{-h}^0 \bar{c} dz \quad (9)$$

$$\phi \equiv -w_s \bar{c} |_{-h} + \overline{w'c'} |_{-h}. \quad (10)$$

The specification of this boundary condition is a major source of uncertainty for sediment transport studies. In the present model a parameterization for ϕ was selected that is similar to expressions used by others (e.g. Lam and Jacquet 1976; Sheng and Lick 1979; Somlyódy 1982; Aalderink et al. 1985; Lavelle et al. 1984). Defining

$$\beta \equiv \frac{w_s \bar{c} |_{-h}}{\tilde{c}} \quad (11a)$$

and

$$E \equiv \overline{w'c'} |_{-h} \quad (11b)$$

and substituting these into Eq. 10 gives

$$\phi = -\beta \tilde{c} + E. \quad (12)$$

The term $\beta \tilde{c}$ in Eq. 12 is the downward sediment flux due to settling. Equation 11a indicates that β is equal to the settling velocity multiplied by a factor that depends on the vertical distribution of sediment suspended in the water column. (For very small particles, $< 1 \mu\text{m}$, the effects of Brownian motion should also be included in β , Lick 1982.) Since the suspended sediment concentration remains nearly uniform over

depth in Lake Balaton, it is expected that $\beta \approx w_s$.

E is parameterized as a function of excess bottom stress.

$$E = 0 \quad \tau < \tau_c \quad (13a)$$

$$E = \beta K \left(\frac{\tau - \tau_c}{\tau_{\text{ref}}} \right)^n \quad \tau \geq \tau_c \quad (13b)$$

τ_{ref} has been included to make the term in parentheses dimensionless.

There is no rigorous theoretical justification of the power law in Eq. 13b as the correct functional form for E . However, it does seem to adequately reproduce measurements of E for both cohesive and non-cohesive sediments (see Lavelle et al. 1984; Lavelle and Mofjeld 1987; Luettich 1987).

Defining

$$c_e \equiv 0 \quad \tau < \tau_c \quad (14a)$$

$$c_e \equiv K \left(\frac{\tau - \tau_c}{\tau_{\text{ref}}} \right)^n \quad \tau \geq \tau_c \quad (14b)$$

allows Eq. 12 to be written as

$$\phi = -\beta(\tilde{c} - c_e) \quad (15)$$

and therefore Eq. 8 becomes

$$\frac{d\tilde{c}}{dt} = -\frac{\beta}{h} (\tilde{c} - c_e). \quad (16)$$

From Eq. 16 it is clear that in this model the depth-averaged concentration is continuously driven toward an equilibrium value defined by Eq. 14a, b. Because τ is variable in time, c_e also varies in time.

The suspended sediment concentration rarely dropped below ~ 15 mg liter $^{-1}$ during the 15-d measurement period (Fig. 3). This "background" concentration can be attributed to very small inorganic particles as well as various planktonic species that were at major bloom levels during the measurement period. To reflect this background in the model, a nonsettling background concentration was introduced into Eq. 16

$$\frac{d\tilde{c}}{dt} = -\frac{\beta}{h} (\tilde{c} - c_{\text{bak}} - c_e) \quad (17)$$

where $c_{\text{bak}} = 15$ mg liter $^{-1}$.

As discussed previously it seems appropriate to set $\tau \approx \tau_{\text{wave}}$ in Eq. 14a, b throughout much of the lake. If we use linear wave theory together with Eq. 3, 4, and 5, the maximal wave-induced bottom stress is linearly related to the wave height by

$$\tau_{\text{wave}} = H \left[\rho \frac{(\nu\omega^3)^{1/2}}{2 \sinh kh} \right] \quad (18)$$

where $\omega \equiv 2\pi/T$ and $k \equiv 2\pi/\lambda$. For a constant ω , the substitution of Eq. 18 into Eq. 14a, b yields

$$c_e = 0 \quad H < H_c \quad (19a)$$

$$c_e = K \left[\frac{H - H_c}{H_{\text{ref}}} \right]^n \quad H \geq H_c. \quad (19b)$$

The wave period (and therefore ω) was relatively constant both during a wind event and from one wind event to another (Fig. 4c). Therefore we used Eq. 19a, b rather than Eq. 14a, b to determine c_e . A value of 1 cm was used as H_{ref} , which, with Eq. 18 and assuming $T = 2$ s and $h = 2$ m, is equivalent to $\tau_{\text{ref}} = 0.072$ dyn cm $^{-2}$.

If c_e is constant in time, Eq. 17 has the analytical solution

$$\tilde{c} = c_e + c_{\text{bak}} + (\tilde{c}_i - c_e - c_{\text{bak}}) \cdot \exp \left[\frac{-\beta}{h} (t - t_i) \right] \quad (20)$$

where the initial conditions are $\tilde{c} = \tilde{c}_i$ at $t = t_i$. The solution of Eq. 17 for a time-varying c_e can be obtained from Eq. 20 with a convolution integral if c_e varies smoothly or with a convolution sum if c_e varies discretely. In the present work it was assumed that c_e varied discretely in steps of length Δt . For each time step an average value of H was determined and used to calculate a value of c_e (Eq. 19a, b). Equation 20 was then used to determine the variation of \tilde{c} over the time step taking \tilde{c} and t from the end of the previous time step as \tilde{c}_i and t_i . The resulting solution is identical to that obtained via a convolution sum and is much easier to implement. All of the model results presented below use $\Delta t = 1,800$ s. Sensitivity studies indicated that smaller values of Δt did not alter the solution significantly.

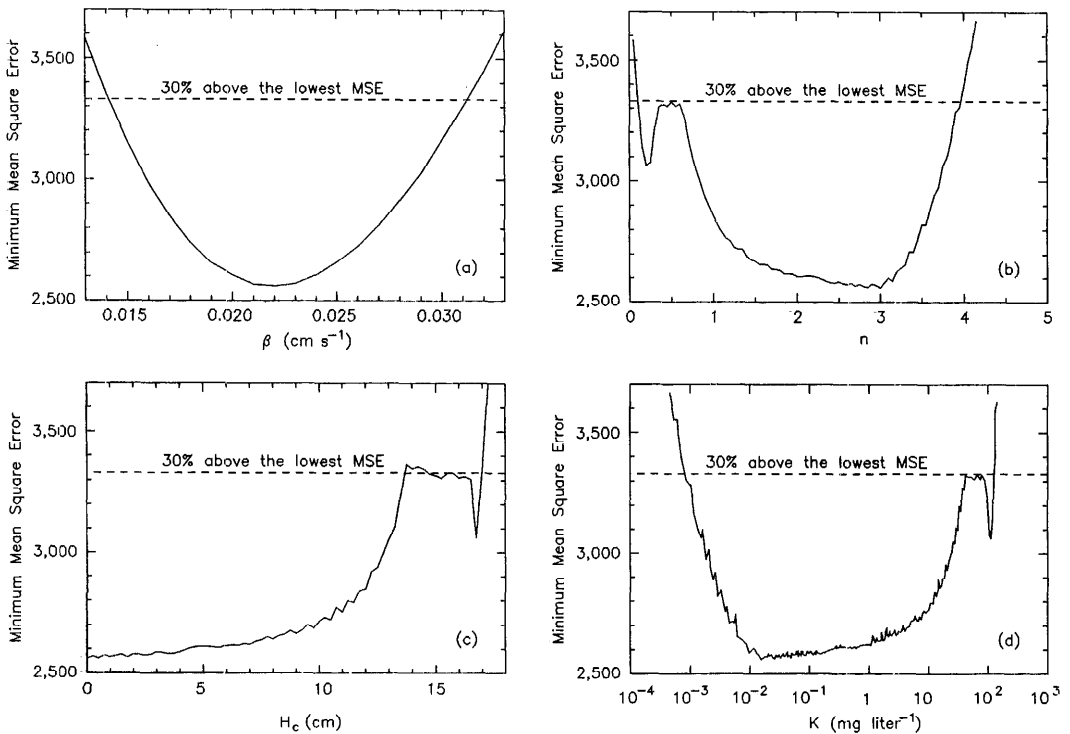


Fig. 6. Minimal MSE as a function of each calibrated parameter when all are allowed to vary independently. (For example panel a shows a projection onto the β -MSE plane of the lower envelope of the minimal MSE surface that exists in four-parameter space. The result is a curve of the minimum MSE as a function of β for all possible combinations of K , n , and H_c .) Horizontal lines represent MSE that is 30% above the lowest value found.

Model calibration and verification

Calibration of the suspended sediment model—The model was calibrated with the significant wave heights and suspended sediment concentrations measured during the second major storm. To do so it was assumed that the middepth measurements were representative of depth-averaged concentrations. The concentration 17.6 mg liter⁻¹ measured at 2145 hours on 17 August was used as the initial condition. Calibration began by systematically and independently varying the parameters K , H_c , β , and n over a wide range of possible values and recording the sum of the mean square error (MSE) between the model predictions and the observed suspended sediment concentrations. Plots of the minimum MSE as a function of each parameter have a well-defined range of parameter values for which the minimum MSE curve is relatively flat

(Fig. 6). Although it might be tempting to select the single parameter set which gave the lowest MSE and call it the optimal model calibration, doing so would ignore any error in the observed data and the fact that the model is only an approximate representation of the system. To allow for these errors, we considered all parameter sets giving MSE values within 30% of the lowest MSE equally acceptable (Table 1). This range

Table 1. Acceptable parameter combinations from model calibration.

MSE	2,560–3,330* mg ² liter ⁻²
H_c	0.0–16.8 cm
β	0.015–0.031 cm s ⁻¹
n	0.15–3.95
K	0.00086–125 mg liter ⁻¹

* 30% variation from the lowest MSE. Specific parameter combinations within the listed ranges yield mean square errors between 2,560 and 3,330.

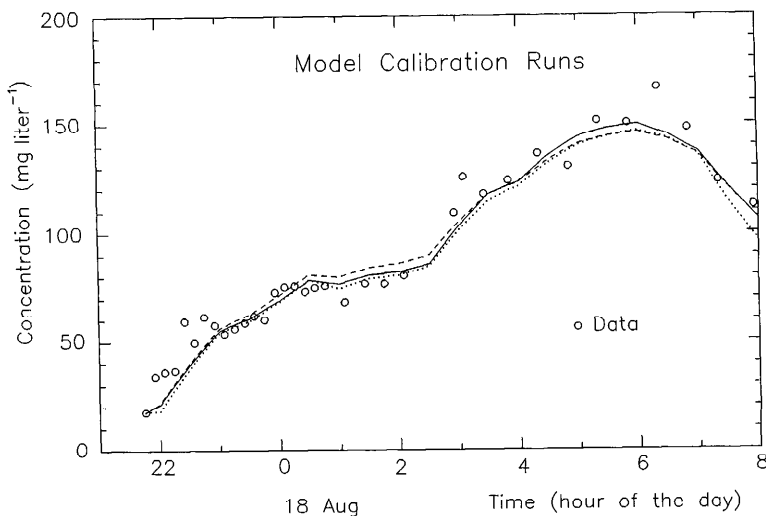


Fig. 7. Comparison between the model and calibration data for three parameter sets. Solid line— $n = 3$; $K = 0.0151 \text{ mg liter}^{-1}$; $\beta = 0.022 \text{ cm s}^{-1}$; $H_c = 0 \text{ cm}$; $\text{MSE} = 2,560 \text{ mg}^2 \text{ liter}^{-2}$; dashed line— $n = 1.75$; $K = 1.19 \text{ mg liter}^{-1}$; $\beta = 0.022 \text{ cm s}^{-1}$; $H_c = 5.92 \text{ cm}$; $\text{MSE} = 2,820 \text{ mg}^2 \text{ liter}^{-2}$; dotted line— $n = 0.88$; $K = 23.5 \text{ mg liter}^{-1}$; $\beta = 0.022 \text{ cm s}^{-1}$; $H_c = 13.4 \text{ cm}$; $\text{MSE} = 3,330 \text{ mg}^2 \text{ liter}^{-2}$.

in MSE was selected arbitrarily and is meaningful only because it includes all parameter values in the flat parts of the curves in Fig. 6. Calibrations with larger and smaller acceptable ranges in MSE yielded increased and decreased limits on the acceptable parameter sets, respectively, but did not significantly affect the parameter covariances.

The wide range of acceptable parameter values (Table 1) indicates either that the model is insensitive to variations in one or more of the parameters or that too many degrees of freedom exist in the model. If it is assumed that $\beta \approx w_s$, however, the values of β are in excellent agreement with the measured settling velocities (Fig. 2). If we assume Stokes' settling law, they correspond to particles in the fine silt size range. To further examine the issue of degrees of freedom, we made a search for covariances between different pairs of parameters from among all of the parameter sets that gave acceptable model calibration. This showed that β was not correlated with any of the other parameters. Therefore a single value could be chosen for β without biasing any of the other parameter values. An average value of $\beta = 0.022 \text{ cm s}^{-1}$ was selected and used in final model runs. On the other hand,

n and K were correlated through the relationship

$$n = -0.67 \log_{10}(K) + 1.8$$

$$r^2 = 0.987. \quad (21)$$

A second set of calibration runs was then made with $\beta = 0.022 \text{ cm s}^{-1}$ and K determined by Eq. 21. From the resulting acceptable parameter sets it was found that n and H_c were correlated through the relationship

$$\log_{10}(n) = -0.040H_c + 0.48$$

$$r^2 = 0.996. \quad (22)$$

If $\beta = 0.022 \text{ cm s}^{-1}$ and Eq. 21 and 22 are substituted into Eq. 20, one free parameter remains that cannot be assigned a unique value from the calibration data. Rather, acceptable model calibrations are obtained for a range of parameter values. Visually, these calibrations are nearly indistinguishable (Fig. 7).

Verification of a wave model—The application of the suspended sediment model requires information about surface waves. A simple model was developed to provide this information (Luettich and Harleman in press) with the shallow-water modifications

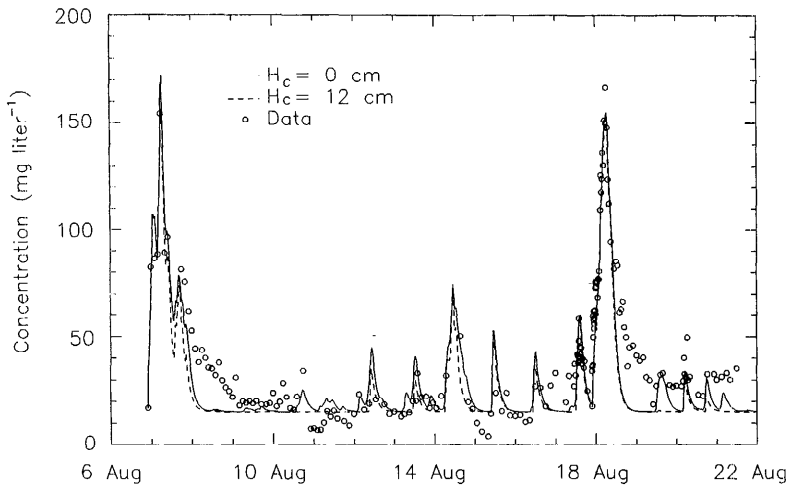


Fig. 8. Comparison between observed suspended sediment concentrations and the model predictions during the 15-d field study.

to the SMB method presented by the CERC (1974). The significant wave height and period are given for fetch-limited waves by the empirical equations:

$$\frac{gH_s}{W_{10}^2} = 0.283 \tanh[\alpha] \tanh\left[\frac{\gamma}{\tanh \alpha}\right] \quad (23)$$

$$\frac{gT}{W_{10}} = 2.8\pi \tanh[\zeta] \tanh\left[\frac{\delta}{\tanh \zeta}\right] \quad (24)$$

$$\alpha = 0.530(gh/W_{10}^2)^{1.75}, \quad (25a)$$

$$\zeta = 0.833(gh/W_{10}^2)^{1.375}, \quad (25b)$$

$$\gamma = 0.0125(gF/W_{10}^2)^{1.42}, \quad (25c)$$

$$\delta = 0.077(gF/W_{10}^2)^{1.25}. \quad (25d)$$

The effective fetch F is defined in the CERC (1974) publication. To use Eq. 23–25 it was assumed that the waves were in local equilibrium with the wind, i.e. that they traveled in the direction of the wind and that the local depth was appropriate for use in Eq. 25a, b. This assumption is reasonable throughout much of the lake because of the gradual changes in water depth. Windspeeds were adjusted up to the required 10 m by assuming a logarithmic velocity profile and using the drag coefficient formula suggested by Wu (1982).

Observed wave heights are reproduced quite well during the two early periods when the winds were blowing along the lake's long axis and during the storm when the winds were oriented across the lake (Fig. 4b,c). The slight overestimation near the beginning of the two events aligned with the lake's long axis suggests that the waves were initially duration rather than fetch limited. During the storm the unsteady nature of the observed wave heights is reproduced reasonably well by the model due to the short cross-lake fetch and therefore the short time required to reach fetch-limited conditions.

Unfortunately, the wave periods were not as well predicted. In order to make the predicted period match the observed period during the main part of each wind event, the leading coefficient in Eq. 24 was adjusted from its value of 2.4 in the original publication (CERC 1974) to 2.8. A more significant problem was that the observations tended to remain nearly constant at a period of about 2 s while the model showed much more variability. From this standpoint a more accurate representation of the observations is obtained by assuming a constant period equal to the average value predicted by the model during the main part of each wind event. Therefore Eq. 19a, b were used rather than 14a, b to model the suspended sediment data.

Verification of the suspended sediment model—The suspended sediment model was verified with a 15-d record of wind and suspended sediment data (Fig. 3). The wave model was used to convert wind velocities into wave heights for the suspended sediment model. The concentration $16.75 \text{ mg liter}^{-1}$ measured at 2200 hours on 6 August was used as the initial condition. H_c was chosen to be the model's free parameter. In general the model does a good job of reproducing observed suspended sediment concentrations during the two major storms, which were oriented across the lake, and during many of the smaller wind events, which were typically oriented along the lake (Fig. 8, Table 2). As indicated in Table 2, a MSE range within 30% of the lowest value can be obtained with H_c varying from 0 to 13 cm. Over the range of H_c from 0 to 8 cm, the model results are nearly indistinguishable, and the MSE varies by $<1.5\%$.

The only systematic deviations between the model and the observations follow the two major storms, when predicted concentrations decrease more rapidly than observed concentrations. As discussed previously, horizontal transport was neglected in the model and therefore may be an explanation for the discrepancy since a relatively long period is associated with particle settling. Györke (unpubl. rep.) found less than a factor of two difference in suspended sediment concentrations across Keszthely Bay during a storm, however, which suggests that the effects of horizontal transport should be small. A more likely explanation for the model discrepancy is differential settling. Because larger particles settle faster than smaller ones, the average settling velocity should decrease during prolonged periods of deposition. This time variation is exactly what the observations appear to show. We note that if a reduced settling rate is taken into account, the model agrees more closely with observations even during several small wind events that occur shortly after each major storm.

Because it was not possible to select a single value for each of the model parameters from either the calibration or verification data sets, several efforts were made to extrapolate values from the literature.

Table 2. Summary of results for varying H_c with verification data.

H_c (cm)	C_{bak} (mg liter ⁻¹)	β (cm s ⁻¹)	n — Eq. 22	K —Eq. 21 (mg liter ⁻¹)	MSE (mg ² liter ⁻²)
0.0	15	0.022	3.02	0.0148	34,400
2.0	15	0.022	2.51	0.0855	34,400
4.0	15	0.022	2.09	0.368	34,300
6.0	15	0.022	1.74	1.24	34,300
8.0	15	0.022	1.45	3.40	34,800
10.0	15	0.022	1.20	7.88	37,000
12.0	15	0.022	1.00	15.9	40,500
13.0	15	0.022	0.91	21.5	43,800
14.0	15	0.022	0.83	28.3	48,200

Stokes' settling law gives $w_s = 0.022 \text{ cm s}^{-1}$ for a particle diameter of $16 \mu\text{m}$. Extensions of Shields' curve for small particles by Mantz (1977) and Miller et al. (1977) suggest a critical stress of $\tau_c \sim 0.5 \text{ dyn cm}^{-2}$. Using Eq. 18 and assuming waves of 2-s periods gives $H_c \sim 7 \text{ cm}$ —well within the range of values for which the model is calibrated.

Alternatively Lavelle et al. (1984) and Lavelle and Mofjeld (1987) argued that τ_c (and therefore H_c) should be zero. Their arguments are based on the highly subjective way in which critical stresses have been determined in laboratory experiments, the stochastic nature of bottom stresses and particle movement, and the fact that previous experimental results, which were originally interpreted with a nonzero critical shear stress, can also be represented with $\tau_c = 0$. For the present model the choice of $H_c = 0$ is clearly consistent with the model calibration (see Fig. 6c) and with the model verification.

Assuming $\tau_c = 0$, Lavelle et al. (1984) reanalyzed erosion rates obtained from several laboratory experiments with fine-grained sediments and found values of n ranging from 1.2 to 5 and values of the rate coefficient ranging from 1.9×10^{-9} to $3.7 \times 10^{-6} \text{ g cm}^{-2} \text{ s}^{-1}$. Using $H_c = 0$ in Eq. 21 and 22 gives $n = 3.0$ and $K = 0.015 \text{ mg liter}^{-1}$. Substituting into Eq. 13b along with $\tau_{\text{ref}} = 0.072 \text{ dyn cm}^{-2}$ yields

$$E = 3.3 \times 10^{-10} (\tau / \tau_{\text{ref}})^3 = 9 \times 10^{-7} \tau^3 \text{ g cm}^{-2} \text{ s}^{-1}. \quad (26)$$

Both the exponent $n = 3$ and rate coefficient fall within the ranges found by Lavelle et

al. (1984), confirming that $H_c = 0$ is also a plausible result.

In summary, the calibration and verification results suggest that it is possible to successfully model the transient behavior of the suspended sediment concentration at our field site with the boundary condition expressed in Eq. 12 and 19. Due to the form of this boundary condition, however, if a small range is allowed in acceptable model behavior, a rather large range can be obtained in acceptable model parameters. We anticipate that a similar conclusion would also apply to the analysis of data from laboratory studies of fine sediment erosion. Therefore it is not surprising that Lavelle et al. (1984) and Lavelle and Mofjeld (1987) were able to fit laboratory experiments with erosion expressions having $\tau_c = 0$ that were originally interpreted with a nonzero τ_c .

The role of cohesiveness in the suspended sediment model

The measured particle settling velocities along with the muddy character of the bottom suggested that the sediments at the study site would be cohesive and therefore that the parameterization used to close Eq. 10 should reflect this property. For convenience, cohesion is generically used to describe both cohesive and adhesive bonding between particles.

Laboratory studies have shown that the erosion and deposition of cohesive sediments are different and exclusive processes. Erosion occurs from a cohesive sediment bed until the depth is reached where the bed strength is equal to the erosive force (Mehta and Partheniades 1979). The bed strength depends on the amount of consolidation that has occurred since the bed was deposited, the make-up of the bed, the temperature, the chemistry of the overlying water and the pore fluid, and bioturbation and secretions by benthic organisms (Southard et al. 1971; Fukuda and Lick 1980; Lee et al. 1981; Parchure and Mehta 1985). Deposition takes place when the applied stress is unable to resuspend or break apart particles or flocs that settle to the bed. It depends on the initial concentration of sediment in suspension, the physicochemical properties of the

sediment in suspension, and the applied stress (Mehta and Partheniades 1975).

Sediment cohesiveness can be included in the bottom flux boundary condition, Eq. 15, via the appropriate definition of c_e (Luettich 1987). In this case, however, c_e will depend on the cohesiveness of the sediment bed and therefore its magnitude (for the same applied stress) will vary in time as the bed consolidates. In addition its functional form will be different depending on whether the bed is eroding or accumulating.

In the model results presented above, c_e was determined by an expression whose form and parameters remained constant in time. As a result, the sediment was being treated as if it were noncohesive. Yet, there were no indications from model behavior that this treatment was unsatisfactory. Although it might be possible that the omission of cohesive effects caused the deviation between the model and the observations during poststorm deposition periods, this interpretation seems unlikely because the model matched the observations quite closely during the initial stages of deposition. Only after 60% or more of the sediment had left suspension did the discrepancy occur.

As a result, the following paradox is suggested: the sediment character suggests that it was cohesive, but the suspended sediment concentration could be modeled as if the sediment was noncohesive. We note that the same paradox applies to the work of Lam and Jacquet (1976), Sheng and Lick (1979), Somlyódy (1982), Aalderink et al. (1985), and Lavelle et al. (1984), all of whom modeled sediment that was presumably cohesive with boundary conditions which treated it as noncohesive.

One explanation is that all of the models simply do a good job of curve fitting. Since it is not our purpose here to assess the success of the other models, our remarks are restricted to the present model. As developed and applied in the preceding sections, the present model is closely based on the physics of the system and has relatively few adjustable parameters. These parameters have been objectively calibrated and verified with independent data sets, with the

verification data including winds blowing both across and along the axis of the lake. The calibrated value of β is in excellent agreement with expected values of w_s based on the particle size distribution, and the resulting parameter values agree with those obtained from laboratory measurements of fine sediment erosion. The only systematic deviation between the model and observations is plausibly explained by differential settling which is not included in the model. Therefore, we feel that the present model does more than coincidentally represent the system behavior.

Another explanation is that the sediments do behave as if they are noncohesive. We speculate that this behavior is the result of a thin layer of sediments that exists at the surface of the sediment bed and whose contents never become cohesively bound to the bed. The thickness of this noncohesive layer may be very small since a suspended sediment concentration of $200 \text{ mg liter}^{-1}$ in a 2-m water column can be obtained by suspending an 0.8-mm-thick sediment layer that has a 95% water content. Possible mechanisms for keeping this layer from becoming part of the bed include bioturbation due to benthic animals and shear associated with the mean current. Although the latter is small in comparison with that due to the waves, it remains relatively constant in time due to the continuous seiche motion of the lake. Also, there may be times that wave action is enough to agitate the surface sediment but not strong enough to resuspend it into the water column. Drake and Cacchione (1986) have found that observations of fine sediment resuspension in Norton Sound, Alaska, and on the northern California shelf also suggest the presence of a surface layer of cohesionless sediment.

Conclusions

The results of the field investigation carried out in Lake Balaton show that episodic increases in the suspended sediment concentration are forced by wind-generated surface waves. Although data were presented from only one field site, the shallowness of the entire lake and the generally comparable magnitude of wave-induced

bottom orbital velocities and mean current velocities suggests that the results will generalize to much of the lake. The most probable exception would occur near Tihany Straits, where large mean currents are known to exist.

Assuming a local equilibrium between wind and waves, it was possible to do a good job of modeling significant wave heights at the field site with a fetch-limited model based on the shallow-water modifications to the SMB method presented by the CERC (1974). This model was not as successful at predicting wave periods, although it did give a reasonable average wave period during substantial wind events. Due to the gradual bottom slope of the lake, it is expected that this model can be used throughout much of the lake.

Observed middepth suspended sediment concentrations could be predicted at the field site over the 15-d study period with a model for the depth-integrated suspended sediment concentration. The model neglected vertical variations in the suspended sediment concentration, horizontal transport, and temporal variations in the particle size distribution and assumed that wave-induced bottom stress was the principal forcing for sediment resuspension. A calibration of the four model parameters to 10 h of data collected during the second major storm yielded ranges of acceptable parameter values comparable with those obtained from laboratory settling velocity measurements and previous laboratory studies of fine sediment erosion. After removing parameter covariances, one free parameter remained in the model for which a definitive value could not be selected based on the calibration data, the 15-d data set used for model verification, or information available in the literature.

The relatively small variation in model results for a large variation in parameter values is consistent with the results of Lavelle et al. (1984) and Lavelle and Mofjeld (1987) who were able to fit expressions having zero critical stress to data that had previously been interpreted with a nonzero critical stress. For this reason we recommend not using modeled suspended sedi-

ment concentrations as a basis for determining values of critical stress.

It is often suggested that the inability to determine a single set of parameter values, as experienced above, indicates that a model contains too many parameters and therefore that one or more parameter can be eliminated. It is not clear, however, in the present case that this suggestion is valid. The elimination of H_c is equivalent to setting it equal to zero. Since $H_c = 0$ may not be physically reasonable, the present model was left with the free parameter. The only systematic model deviation from observed data was toward the end of periods of prolonged deposition and was most likely caused by omission of differential settling from the model.

It was possible to do a good job modeling the suspended sediment concentration assuming that the sediment was noncohesive despite the fact that the sediment characteristics suggested otherwise. We speculate that while the major portion of the sediment bed may be cohesive, a thin layer of sediment particles exists at the bed surface that is kept from becoming part of the bed by bioturbation and bottom shear exerted by the mean current and small waves. Although the latter may be weak in comparison to the stress necessary to cause resuspension, it is almost always present in the lake.

The results of the present study can be applied in two contexts. First, where the assumptions of local equilibrium with the wind and negligible horizontal transport are valid, the model developed herein is simple enough to be easily integrated into a water-quality model. We expect that parameter values will vary if the model is applied over different sediment types and therefore several sets of parameter calibrations may have to be made for a water-quality model of an entire lake. Second, a more general model of suspended sediment transport, which may include horizontal transport as well as other complicating features, requires the same information on bottom boundary conditions as the present model. Therefore, the results of the present study can be used to specify this boundary condition, although we again

expect that different sediment types may require parameter values to be recalibrated.

References

- AALDERINK, R. H., L. LIJKLEMA, J. BREUKELMAN, W. VAN RAAPHORST, AND A. G. BRINKMAN. 1985. Quantification of wind induced resuspension in a shallow lake. *Water Sci. Technol.* **17**: 943-954.
- ANDERSON, F. E. 1972. Resuspension of estuarine sediments by small amplitude waves. *J. Sediment. Petrol.* **42**: 602-607.
- CARPER, G. L., AND R. W. BACHMANN. 1984. Wind resuspension of sediments in a prairie lake. *Can. J. Fish. Aquat. Sci.* **41**: 1763-1767.
- CERC. 1974. Shore protection manual. V. 1. U.S. Army Coastal Eng. Res. Center, Ft. Belvoir, Va.
- DRAKE, D. E., AND D. A. CACCHIONE. 1986. Field observations of bed shear stress and sediment resuspension on continental shelves, Alaska and California. *Cont. Shelf Res.* **6**: 415-429.
- DYER, K. R. 1986. Coastal and estuarine sediment dynamics. Wiley.
- FUKUDA, M. K., AND W. LICK. 1980. The entrainment of cohesive sediments in freshwater. *J. Geophys. Res.* **85**: 2813-2824.
- GELENCSE, P., F. SZILÁGYI, L. SOMLYÓDY, AND L. LIJKLEMA. 1982. A study on the influence of sediment in the phosphorus cycle in Lake Balaton. *Int. Inst. Appl. Syst. Anal. Collaborative Pap.* CP-82-44.
- GRANT, W. D., AND O. S. MADSEN. 1979. Combined wave and current interactions with a rough bottom. *J. Geophys. Res.* **84**: 1797-1808.
- GROSS, T. F., A. J. WILLIAMS III, AND W. D. GRANT. 1986. Long-term in situ calculations of kinetic energy and Reynolds stress in a deep sea boundary layer. *J. Geophys. Res.* **91**: 8461-8469.
- HAWLEY, N. 1983. A numerical model of cohesive suspended sediment dynamics. NOAA Tech. Memo. GLERL-42.
- KAMPHIUS, J. W. 1975. Friction factor under oscillatory waves. *J. Waterways Harbors Coastal Eng. Div. (Am. Soc. Civ. Eng.)* **101**: 135-144.
- LAM, D. C. L., AND J.-M. JACQUET. 1976. Computations of physical transport and regeneration of phosphorus in Lake Erie, fall 1970. *J. Fish. Res. Bd. Can.* **33**: 550-563.
- LÁNG, I. 1986. Impact of policy making: Background to a government decision, p. 110-121. *In* L. Somlyódy and G. van Straten [eds.], *Modelling and managing shallow lake eutrophication with application to Lake Balaton*. Springer.
- LAVELLE, J. W., AND H. O. MOFJELD. 1987. Do critical stresses for incipient motion and erosion really exist? *J. Hydraul. Eng. (Am. Soc. Civ. Eng.)* **113**: 370-385.
- , ———, AND E. T. BAKER. 1984. An in situ erosion rate for fine-grained marine sediment. *J. Geophys. Res.* **89**: 6543-6552.
- LEE, D.-Y., W. LICK, AND S. W. KANG. 1981. The entrainment and deposition of fine-grained sedi-

- ment in Lake Erie. *J. Great Lakes Res.* **7**: 224–233.
- LESHT, B. M., T. L. CLARKE, R. A. YOUNG, D. J. P. SWIFT, AND G. L. FREELAND. 1980. An empirical relationship between the concentration of resuspended sediment and near bottom wave-orbital velocity. *Geophys. Res. Lett.* **7**: 1049–1052.
- LICK, W. 1982. Entrainment, deposition and transport of fine-grained sediments in lakes. *Hydrobiologia* **91**: 31–40.
- . 1986. Modeling the transport of fine-grained sediments in aquatic systems. *Sci. Total Environ.* **55**: 219–228.
- LIJKLEMA, L., P. GLENCSEER, F. SZILÁGYI, AND L. SOMLYÓDY. 1986. Sediment and its interaction with water, p. 156–182. *In* L. Somlyódy and G. van Straten [eds.], *Modelling and managing shallow lake eutrophication with application to Lake Balaton*. Springer.
- LUETTICH, R. A., JR. 1987. Sediment resuspension in a shallow lake. D.S. thesis, Mass. Inst. Technol., Cambridge. 311 p.
- , AND D. R. F. HARLEMAN. 1986. A comparison of water quality models and load reduction predictions, p. 323–340. *In* L. Somlyódy and G. van Straten [eds.], *Modelling and managing shallow lake eutrophication with application to Lake Balaton*. Springer.
- , AND ———. *In press*. A comparison between measured wave properties and simple wave hindcasting models in shallow water. *J. Hydraul. Res.*
- MCLEAN, S. R. 1985. Theoretical modelling of deep ocean sediment transport. *Mar. Geol.* **66**: 243–265.
- MANTZ, P. A. 1977. Incipient transport of fine grains and flakes by fluids—extended Shields diagram. *J. Hydraul. Div. (Am. Soc. Civ. Eng.)* **103**: 601–615.
- MEHTA, A. J., AND E. PARTHENIADES. 1975. An investigation of the depositional properties of flocculated fine sediments. *J. Hydraul. Res.* **13**: 361–381.
- , AND ———. 1979. Kaolinite resuspension properties. *J. Hydraul. Div. (Am. Soc. Civ. Eng.)* **105**: 411–416.
- MILLER, M. C., I. N. MCCAVE, AND P. D. KOMAR. 1977. Threshold of sediment motion under unidirectional currents. *Sedimentology* **24**: 507–527.
- MONIN, A. S., AND A. M. YAGLOM. 1971. *Statistical fluid mechanics*. V. 1. MIT.
- OCHI, M. K. 1982. Stochastic analysis and probabilistic prediction of random seas. *Adv. Hydrosci.* **13**: 217–374.
- PARCHURE, T. M., AND A. J. MEHTA. 1985. Erosion of soft cohesive sediment deposits. *J. Hydraul. Eng. (Am. Soc. Civ. Eng.)* **111**: 1308–1326.
- SHANAHAN, P., AND D. R. F. HARLEMAN. 1982. Linked hydrodynamic and biogeochemical models of water quality in shallow lakes. Ralph M. Parsons Lab., Mass. Inst. Technol. Tech. Rep. 268.
- SHENG, Y. P., AND W. LICK. 1979. The transport and resuspension of sediments in a shallow lake. *J. Geophys. Res.* **84**: 1809–1826.
- SLEATH, J. F. A. 1984. *Sea bed mechanics*. Wiley.
- SMITH, J. D. 1977. Modelling of sediment transport on continental shelves, p. 539–577. *In* E. D. Goldberg et al. [eds.], *The sea*. V. 6. Wiley-Interscience.
- SOMLYÓDY, L. 1982. Water-quality modelling: A comparison of transport-oriented and ecology-oriented approaches. *Ecol. Model.* **17**: 183–207.
- , AND G. VAN STRATEN. 1986. *Modelling and managing shallow lake eutrophication with application to Lake Balaton*. Springer.
- SOULSBY, R. L. 1983. The bottom boundary layer of shelf seas, p. 189–266. *In* B. Johns [ed.], *Physical oceanography of coastal and shelf seas*. Elsevier.
- SOUTHARD, J. B., R. A. YOUNG, AND C. D. HOLLISTER. 1971. Experimental erosion of calcareous ooze. *J. Geophys. Res.* **76**: 5903–5909.
- VAN LEUSSEN, W. 1986. Laboratory experiments on the settling velocity of mud flocs, p. 1803–1812. *In* Proc. 3rd Int. Symp. River Sedimentation. Univ. Mississippi.
- WILLIAMS, A. J., III. 1985. BASS, an acoustic current meter array for benthic flow-field measurements. *Mar. Geol.* **66**: 345–355.
- WU, J. 1982. Wind-stress coefficients over sea surface from breeze to hurricane. *J. Geophys. Res.* **87**: 9704–9706.

Submitted: 23 February 1989

Accepted: 21 February 1990

Revised: 30 April 1990